

---

# SAFE OPTIMAL CONTROL UNDER PARAMETRIC UNCERTAINTIES

---

PREPRINT

**Hemanth Sarabu\***  
Symbio Robotics  
hemanth@symb.io

**Venkata Ramana Makkapati\***  
Georgia Tech  
mvramana@gatech.edu

**Vinodhini Comandur\***  
Georgia Tech  
vinodhini@gatech.edu

**Panagiotis Tsiotras**  
Georgia Tech  
tsiotras@gatech.edu

**Seth Hutchinson**  
Georgia Tech  
seth@gatech.edu

October 19, 2022

## ABSTRACT

We address the issue of safe optimal path planning under parametric uncertainties using a novel regularizer that allows trading off optimality with safety. The proposed regularizer leverages the notion that collisions may be modelled as constraint violations in an optimal control setting to produce open-loop trajectories with reduced risk of collisions. The risk of constraint violation is evaluated using a state-dependent *relevance function* and first-order variations in the constraint function with respect to parametric variations. The approach is generic and can be adapted to any optimal control formulation that deals with constraints under parametric uncertainty. Simulations using a holonomic robot with simple dynamics avoiding multiple dynamic obstacles with uncertain velocities are used to demonstrate the effectiveness of the proposed approach. Finally, we introduce the *car vs. train problem* to emphasize the dependence of the resultant risk aversion behavior on the form of the constraint function used to derive the regularizer.

## 1 Introduction

The tension between optimality and safety often appears in robotics—particularly for applications that have stringent performance requirements—under conditions for which uncertainties in sensing, environment models, and control effectiveness are unavoidable [23, 8, 10, 11]. For all but the simplest applications, optimal solutions tend to bring the robot dangerously close to operational safety margins. For example, it is well known that the shortest path for a mobile robot in a polygonal environment lies in the visibility graph which implies that the optimal path would contact the obstacles while traversing the path. While in practice, it is typical to perturb paths slightly such that they do not reach the constraint boundaries, it raises a number of significant questions: How should one perform these perturbations? How should one balance the cost of violating constraints against reduced performance? And, perhaps most importantly, how can one provide a principled evaluation of the effects of uncertainty with respect to the trade-offs between optimality and safety, and adjust the path to optimally balance between the two? It is this latter question that we address in the present paper.

Our approach exploits recent results in the area of desensitized optimal control (DOC) [14, 13]. DOC techniques modify the nominal optimal trajectory such that it is *less sensitive* with respect to uncertain parameters. This involves constructing an appropriate sensitivity cost which, when penalized, provides solutions that are relatively insensitive to parametric uncertainties. Primarily, DOC methods take a global view of parametric uncertainty, attempting to provide robust solutions along the entire trajectory [13, 18]. In contrast, we consider explicitly the effects of parametric uncertainty for those portions of the trajectory that approach (or contact) constraint boundaries, essentially ignoring

---

\*Equal contributions (listed alphabetically)

parametric uncertainties for states that are inherently safe even under large parametric variations. In this way, we focus both computation and control effort on those areas that are most crucial for overall system safety.

Formally, we consider uncertainties to be parametric in nature, where the nominal value of the uncertain parameter is available. Using sensitivity functions [9], we first capture the variations in the constraint function under parametric variations. The variations are then weighted using a relevance function to construct a regularizer that captures the risk of constraint violation. The characteristics of the regularizer are discussed by analyzing its performance in simple path planning problems. Finally, we evaluate the proposed technique on path planning problems in environments containing up to ten dynamic obstacles with uncertainties in their velocities.

Probabilistic methods is a popular choice to address planning in uncertain dynamic environments [19]. In the past, Gaussian processes have been employed to model uncertainty and to obtain safe trajectories [3, 22, 21, 1]. Techniques involving POMDPs [12, 24], occupancy grids [7], intent-based threat estimation [2], replanning [20, 25], and feedback coupled with estimation [5] are many variants in the class of probabilistic methods. Alternatively, reachability analysis [6, 4], artificial potential fields (APFs) [15] and barrier functions [17] have also been utilized. Our approach fundamentally differs from the above techniques in its formulation; while prior work widely employed probabilistic techniques, the proposed formulation is deterministic. In order to address planning under limited sensing and feedback capabilities, we provide safe open-loop trajectories that have guarantees on optimality by treating the uncertainty to be parametric in nature, and examining the first-order variations.

The rest of the paper is organized as follows. Section 2 introduces sensitivity functions and the framework of DOC. Section 3 presents the main idea of the paper, involving the construction of an appropriate regularizer that provides open-loop trajectories with lower chance of constraint violation under parametric uncertainties. In Section 4, we analyze the proposed approach by applying it on simple path planning problems with one dynamic obstacle. Section 5 presents the results obtained from experiments on environments with multiple uncertain dynamic obstacles. Section 6 concludes the paper.

## 2 Preliminaries

### 2.1 Standard Optimal Control Framework

Consider the standard optimal control problem of minimizing the cost

$$\mathcal{J}(u) = \phi(x(t_f), t_f) + \int_{t_0}^{t_f} L(x(t), u(t), t) dt, \quad (1)$$

subject to

$$\dot{x}(t) = f(x(t), p, u(t), t), \quad x(t_0) = x_0, \quad (2)$$

$$g(x(t), p, t) \leq 0, \quad (3)$$

where  $t \in [t_0, t_f]$  denotes time, with  $t_0$  being the fixed initial time and  $t_f$  being the final time,  $x(t) \in \mathbb{R}^n$  denotes the state, with  $x_0$  being the fixed state at  $t_0$ , and  $p \in \mathcal{P} \subset \mathbb{R}^\ell$  are model parameters. The control  $u \in \mathcal{U} = \{\text{Piecewise Continuous (PWC)}, u(t) \in U, \forall t \in [t_0, t_f]\}$  with  $U \subseteq \mathbb{R}^m$ , the set of allowable values of  $u(t)$ ,  $\phi: \mathbb{R}^n \times [t_0, t_f] \rightarrow \mathbb{R}$ , the terminal cost function, and  $L: \mathbb{R}^n \times \mathbb{R}^m \times [t_0, t_f] \rightarrow \mathbb{R}$ , the running cost. Finally,  $g: \mathbb{R}^n \times \mathbb{R}^\ell \times [t_0, t_f] \rightarrow \mathbb{R}^k$  is a function denoting  $k$  state inequality constraints. Let

$$\psi(x(t_f), t_f) = 0, \quad (4)$$

be the terminal condition at time  $t = t_f$ .

The aforementioned problem is to be solved by finding the optimal control  $u^* \in \mathcal{U}$  that minimizes the cost function in (1), given the constraints (2)-(4). The solution defines the optimal state trajectory  $x^*(t)$ ,  $t \in [t_0, t_f]$ , satisfying  $\dot{x}^*(t) = f(x^*(t), p, u^*(t), t)$  subject to  $x^*(t_0) = x_0$ . The system dynamics in (2) represented by the function  $f(x, p, u, t)$  contains the model parameters,  $p \in \mathcal{P}$ , which are assumed to be constant. In general, the optimal solution  $(x^*(t), u^*(t))$  is sensitive to modeling errors and, if changes in the parameters  $p$  occur at any time  $t \in [t_0, t_f]$ , satisfaction of the constraint (3) is not guaranteed.

In the case of path planning with dynamic obstacles, collision avoidance is of paramount importance. Obtaining safe trajectories under parametric uncertainties in the obstacles' motion is a necessity. In the optimal control framework discussed above, the constraint function in (3) can be used to enforce collision avoidance for the path planning problem. Consequently, obtaining and penalizing a risk measure that captures the possibility of constraint violation under parametric variations may provide the desired safe (e.g., lower chance of constraint violation) trajectories.

With the motivation to minimize the dispersion in the optimal trajectory under parameter uncertainties, an augmented cost function using sensitivity functions has been constructed in [13]. In this paper, sensitivity functions are used to impose the desired risk measure for constraint violation. To this end, we first discuss the approach in [13] along with the theory behind the sensitivity functions in the following subsection.

## 2.2 Sensitivity Functions and DOC

Consider the dynamics in (2), and assume variations in the model parameters  $p \in \mathcal{P}$ , with  $p = p_0$  being the nominal value of the parameter vector. Furthermore, assume that  $f(x, p, u, t)$  is continuous in  $(x, p, u, t)$ , and continuously differentiable with respect to  $x$  and  $p$  for all  $(x, p, u, t) \in \mathbb{R}^n \times \mathcal{P} \times U \times [t_0, t_f]$ . The solution to the differential equation from the initial condition  $x_0$  with control input  $u \in \mathcal{U}$  is given by

$$x(p, t) = x_0 + \int_{t_0}^t f(x(p, \tau), p, u(\tau), \tau) d\tau. \quad (5)$$

Since  $f(x, p, u, t)$  is differentiable with respect to  $p$ , it follows

$$\frac{\partial x}{\partial p}(p, t) = \int_{t_0}^t \left[ \frac{\partial f}{\partial x}(x(p, \tau), p, u(\tau), \tau) \frac{\partial x}{\partial p}(p, \tau) + \frac{\partial f}{\partial p}(x(p, \tau), p, u(\tau), \tau) \right] d\tau. \quad (6)$$

Taking the derivative with respect to  $t$ , we obtain

$$\frac{d}{dt} \left[ \frac{\partial x}{\partial p}(p, t) \right] = \frac{\partial f(x, p, u(t), t)}{\partial x} \Big|_{x=x(p, t)} \frac{\partial x}{\partial p}(p, t) + \frac{\partial f(x, p, u(t), t)}{\partial p} \Big|_{x=x(p, t)}. \quad (7)$$

Evaluating (7) at the nominal conditions ( $p = p_0$ ), the dynamics for the *parameter sensitivity function*

$$S(t) = \frac{\partial x(p, t)}{\partial p} \Big|_{x=x(p_0, t)} \quad (8)$$

can be obtained as

$$\dot{S}(t) = A(t)S(t) + B(t), \quad S(t_0) = 0_{n \times \ell}, \quad (9)$$

where

$$A(t) = \frac{\partial f(x, p, u(t), t)}{\partial x} \Big|_{x=x(p_0, t), p=p_0}, \quad (10)$$

$$B(t) = \frac{\partial f(x, p, u(t), t)}{\partial p} \Big|_{x=x(p_0, t), p=p_0}. \quad (11)$$

Since the initial state is given (fixed), the initial condition for the sensitivity function is the zero matrix, and (9) is called the *sensitivity equation* in the literature [9]. To compute the sensitivity function overtime, the state  $x$  has to be propagated using the dynamics in (2) under nominal conditions,

$$\dot{x} = f(x, p_0, u, t), \quad x(t_0) = x_0. \quad (12)$$

From the properties of continuous dependence with respect to the parameters and the differentiability of solutions of ordinary differential equations, for sufficiently small variations in  $p_0$ , the solution  $x(p, t)$  can be approximated by

$$x(p, t) \approx x(p_0, t) + S(t)(p - p_0). \quad (13)$$

This is a first-order approximation of  $x(p, t)$  about the nominal solution  $x(p_0, t)$ .

For the optimal control problem (1)-(4) in the previous subsection, an approach to construct a *desensitized optimal control* (DOC) scheme that reduces the dispersion in the optimal trajectories under parametric uncertainties is to minimize the augmented cost function

$$\mathcal{J}_s(u) = \mathcal{J}(u) + \int_{t_0}^{t_f} \|\text{vec } S(t)\|_Q^2 dt, \quad (14)$$

with an augmented state  $[x^\top (\text{vec } S)^\top]^\top$ , whose dynamics is obtained from (12), (9), and the constraints (3), (4). Here,  $\text{vec } S$  denotes vectorization of the matrix  $S$ . Equation (14) minimizes the original cost function in (1), while penalizing the sensitivity of the state with respect to the parameters along the optimal trajectory. The weighting factor for the sensitivity cost,  $Q \geq 0$ , can be tuned to balance between minimizing the original cost and minimizing the sensitivity cost. In the next section, we develop a scheme to generate constraint desensitized trajectories by penalizing a risk measure that is developed using sensitivity functions.

### 3 Constraint Desensitized Path Planning

For the optimal control problem (1)-(4), assuming the constraint function  $g(x, p, t)$  is a smooth function in  $x$ , a naïve approach to obtain conservative trajectories to address constraint violation under parametric uncertainties would be to penalize

$$S_g(t) = \left. \frac{\partial g(x(p, t), p, t)}{\partial p} \right|_{p=p_0} \quad (15)$$

$$= \left( \frac{\partial h(x, p, t)}{\partial x} S(t) + \frac{\partial g(x, t)}{\partial p} \right) \Big|_{x=x(p_0, t), p=p_0}, \quad (16)$$

by constructing the augmented cost

$$\mathcal{J}(u) + \int_{t_0}^{t_f} \|\text{vec } S_g(t)\|_Q^2 dt, \quad (17)$$

where  $Q \geq 0$ . Note that by minimizing the cost in (17), one attempts to minimize the variation in the constraint value with respect to variations in the parameter for all times. However, it is understood that the variation in the constraint value when it is far from the constraint boundary is not as important as when the constraint value is closer to the boundary. For example, in the case of the path planning problem with dynamic obstacles, a larger variation in the constraint value when the agent is far away from the obstacle is acceptable, but a relatively smaller variation when the agent is near the constraint boundary can be disastrous. Weighting the sensitivity of the constraint value equally in both cases using a running cost function may lead to solutions that are highly sensitive near the constraint boundary. To mitigate this issue, we introduce the logistic function

$$\ell(x) = \frac{1}{1 + e^{-kx}}, \quad (18)$$

where  $k > 0$  is the logistic growth rate. The function derivative of (18) is given by

$$\frac{\partial \ell(x)}{\partial x} = k\ell(x)(1 - \ell(x)). \quad (19)$$

Note that its derivative has a bell shape with the maximum at  $x = 0$ , and decaying tails on both sides. The width of the curve can be adjusted using the growth rate  $k$ . The proposed approach goes as follows. We first consider the composite function  $\ell(g(x, t))$ , and obtain its sensitivity at time  $t$  as

$$\begin{aligned} S_\ell(t) &= \left. \frac{\partial \ell(g(x(p, t), p, t))}{\partial p} \right|_{p=p_0} \\ &= \frac{\partial \ell(g(x(p, t), p, t))}{\partial g} \frac{\partial g(x(p, t), p, t)}{\partial p} \Big|_{p=p_0} \\ &= \underbrace{k\ell(g(x(p, t), p, t)) \left(1 - \ell(g(x(p, t), p, t))\right)}_{\text{relevance term}} \times S_g(t) \Big|_{p=p_0}. \end{aligned} \quad (20)$$

To differentiate between  $S_g$  and  $S_\ell$ , the former is called *constraint sensitivity*, and the latter is called *relevant constraint sensitivity* (RCS). The relevance term in RCS is one of the key ideas of this work, which allows one to penalize sensitivities according to their relevance to potential constraint violation. Note that the logistic function is just one of the many possible functions that can be used to capture the idea of constraint relevance. For example, the penalty function forms used in the interior point methods can also serve in the place of logistic function when tuned appropriately. The sensitivity  $S_\ell(t)$  now captures the idea of giving more importance to the variations near the constraint boundary.

Finally, we propose to solve the optimal control problem with the augmented cost function

$$\mathcal{J}_a(u) = \mathcal{J}(u) + \int_{t_0}^{t_f} \|\text{vec } S_\ell(t)\|_Q^2 dt, \quad (21)$$

the dynamics in (12) and (9), and the constraints (3) and (4) to construct trajectories that address constraint violation under parametric uncertainties. Hereafter, the term  $\int_{t_0}^{t_f} \|\text{vec } S_\ell(t)\|_Q^2 dt$  will be referred to as the RCS cost.

## 4 Numerical Examples

In this section, we apply the proposed approach on simple test examples to analyze the optimal trajectories obtained by penalizing RCS. First, we analyze the claim of penalizing RCS over constraint sensitivity using a 2D path planning problem with a single dynamic obstacle with uncertainty in its speed. Subsequently, the effect of various constraint forms that represent the collision avoidance condition, chosen from a set of valid ones, is studied. Finally, we stress upon the need for selecting an appropriate constraint function to construct RCS using the car vs. train problem.

### 4.1 2D Time-Optimal Problem

Consider the following 2D time-optimal path planning problem with the agent dynamics and initial conditions

$$\dot{x}_a(t) = v_a \cos(\theta(t)), \quad x_a(0) = a_0, \quad (22)$$

$$\dot{y}_a(t) = v_a \sin(\theta(t)), \quad y_a(0) = b_0, \quad (23)$$

where  $(x_a, y_a)$  denotes the agent's position,  $v_a$  is the agent's speed, and  $\theta(t) \in [0, 2\pi)$  is the agent's heading (control). The agent intends to reach  $(a_f, b_f)$  in minimum time, while avoiding a dynamic circular obstacle that is moving parallel to the  $y$ -axis with a constant speed  $v_o$ , and dynamics given by

$$\dot{y}_o(t) = -v_o, \quad y_o(0) = c, \quad (24)$$

where  $(x_o, y_o)$  denotes the obstacle's position. With  $x = [x_a, y_a, y_o]^\top$  as the state vector, the constraint for collision avoidance can be expressed as

$$g(x) = r_o - \sqrt{(x_a(t) - x_o)^2 + (y_a(t) - y_o(t))^2} \leq 0, \quad (25)$$

where  $r_o$  is the safe distance. For this problem, we assume that the obstacle's speed  $v_o$  is the uncertain parameter. Henceforth, the time and parameter dependency of the elements in the state vector are dropped for brevity. Since the problem has simple dynamics, a closed form expression to the sensitivity of the constraint function  $g(x)$  with the respect to the uncertain parameter  $v_o$  is given by

$$\begin{aligned} S_g(t) &= \frac{\partial g(x)}{\partial v_o} = \frac{\partial(r_o - \sqrt{(x_a - x_o)^2 + (y_a - y_o)^2})}{\partial v_o} \\ &= \frac{y_a - y_o}{\sqrt{(x_a - x_o)^2 + (y_a - y_o)^2}} \frac{\partial y_o}{\partial v_o} \\ &= -\frac{(y_a - y_o)t}{\sqrt{(x_a - x_o)^2 + (y_a - y_o)^2}}. \end{aligned} \quad (26)$$

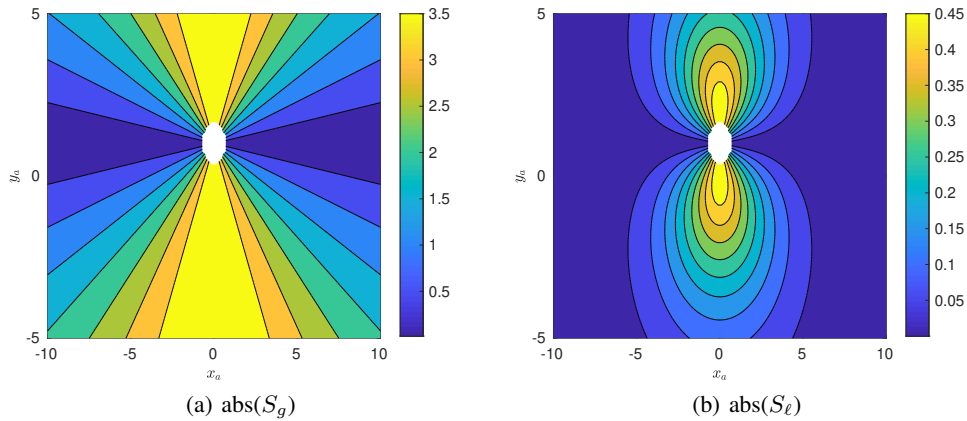


Figure 1: Absolute values of  $S_g$  and  $S_\ell$  as a function of the agent's position.

The effect of incorporating the logistic function into the proposed scheme is analyzed by comparing the constraint sensitivity and RCS. In this regard, the obstacle's position is fixed at  $(0, 1)$  with  $r_o = 0.6$ , and since the constraint sensitivity varies linearly with time,  $t = 1$  is chosen. Figure 1 presents the absolute values of the sensitivities ( $S_g$

and  $S_\ell$ ) over the mesh generated to represent the agent's position. The white circular area in the middle represents the infeasible region. It can be observed that RCS ( $S_\ell$ ) is activated when the agent gets closer to the obstacle, as opposed to the constraint sensitivity, which only captures the sensitivity in the constraint value. Furthermore, it has also been observed (though not presented here for the sake of brevity) that by just penalizing the constraint sensitivity using the cost in (17), conservative trajectories cannot be obtained as the sensitivity profile over-constrains the problem (see Figure 1(a)). In the case of penalizing RCS, the agent has sufficient incentive for moving away from the obstacle as the variations closer to the constraint boundary now incur penalty (see Figure 1(b)).

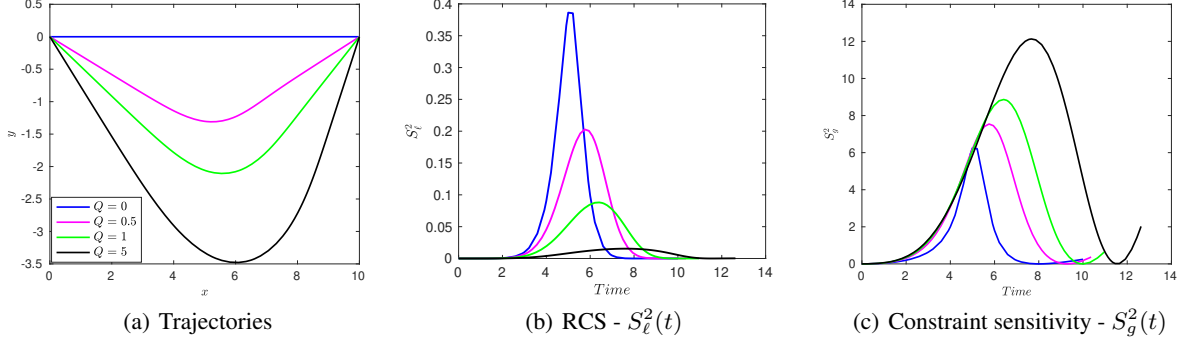


Figure 2: Results for constraint desensitized 2D path planning

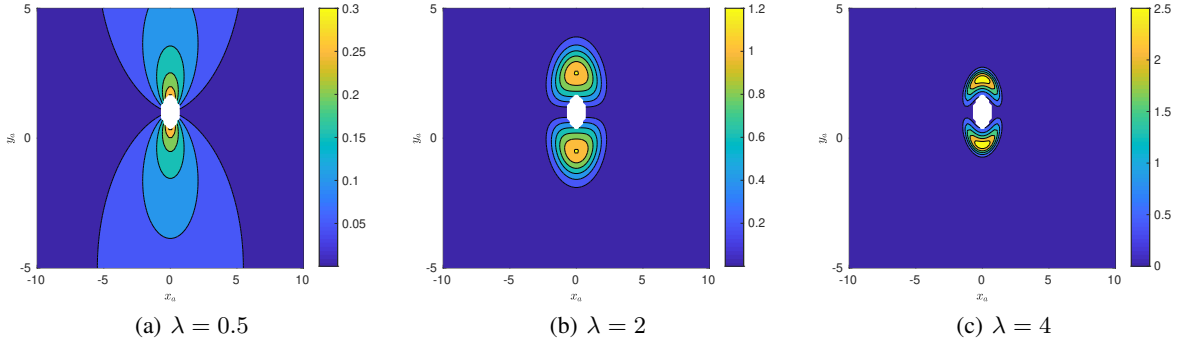


Figure 3: Absolute values of RCS for different constraint forms over the grid representing the agent's position. The white circular area in the middle represents the infeasible region.

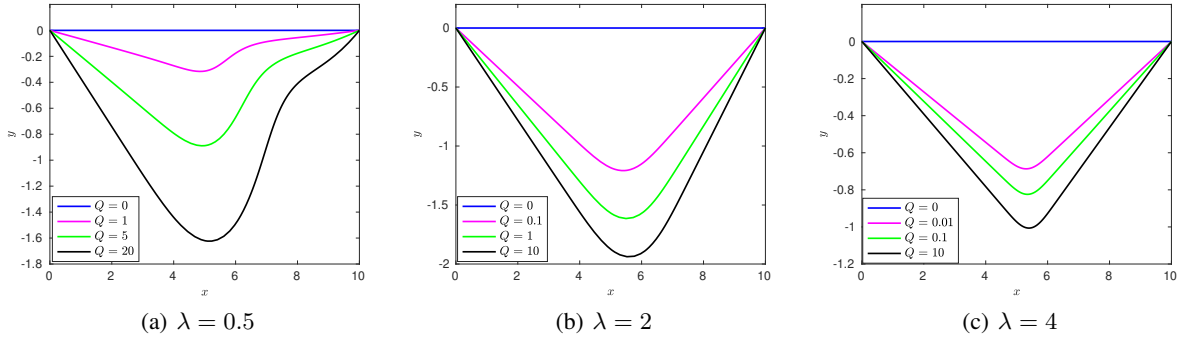


Figure 4: Optimal trajectories for constraint desensitized planning under different constraint forms

Figure 2 shows the results obtained for the previous path planning problem with  $(a_0, b_0) = (0, 0)$ ,  $(a_f, b_f) = (0, 10)$ ,  $x_o = 5$ ,  $c = 2$ , and  $v_a = 1$ . The nominal value of the uncertain parameter  $v_o$  is chosen to be 0.25. The cost function in

(21) is minimized with  $\phi(x(t_f), t_f) = t_f$ ,  $L(x(t), u(t), t) = 0$ , given the dynamics (22)-(24), and the constraint (25). GPOPS-II is used to numerically solve the optimal control problem [16]. From Figure 2(a), it can be observed that as the weighting factor  $Q$  for RCS term in the cost function increases, the optimal trajectory becomes more conservative (the distance to the obstacle is greater) and RCS reduces along the trajectory (see Figure 2(b)). Figure 2(c) suggests that the conservative trajectories have higher constraint sensitivity, and further corroborates the underlying intuition behind introducing the logistic function in (18). A video demonstrating the trajectories along with the obstacle's motion can be found on the web<sup>†</sup>.

## 4.2 Dependency on the Constraint Form

In this section, the effect of the form of the constraint function over the behavior of the optimal trajectories obtained from constraint desensitized planning is observed. To this end, the constraint function in (25) is expressed alternatively as

$$g_\lambda(x) = r_o^\lambda - \left[ \sqrt{(x_a - x_o)^2 + (y_a - y_o)^2} \right]^\lambda \leq 0, \quad (27)$$

where  $\lambda > 0$ . We first analyze the RCS plots shown in Figure 3. The simulation parameters remain the same as the ones used for the results in Figure 1. The general expression for RCS, for any  $\lambda > 0$ , is given by

$$S_\ell = -k \underbrace{L(g_\lambda(x))(1 - L(g_\lambda(x)))}_{\text{relevance term}} \times \underbrace{\lambda(y_a - y_o)t \left[ (x_a - x_o)^2 + (y_a - y_o)^2 \right]^{\lambda/2-1}}_{\text{constraint sensitivity}} \quad (28)$$

Note that, for  $\lambda > 0$ , the relevance term (see (28)) decays exponentially as the agent moves away from the obstacle. For  $\lambda > 2$ , the constraint sensitivity part increases super-linearly with the separation between the agent and the obstacle. Consequently, RCS decays with the Euclidean distance and becomes prominent as the agent gets closer to the obstacle. Also, as  $\lambda$  increases, the decay (logistic) term overpowers the constraint sensitivity term and the penalty region around the obstacle shrinks.

Figure 4 presents the optimal trajectories given the constraint form in (27), for  $\lambda = 0.5, 2, 4$ , with different weights ( $Q$ ) in RCS cost. The videos for the trajectories in Figure 4 along with the obstacle's movements can be found on the web<sup>‡</sup>. The simulation parameters are the same as the ones used for the results in Figure 2. Similar to the results obtained for  $\lambda = 1$ , the optimal trajectories become conservative for all values of  $\lambda$ , as  $Q$  increases (see videos in the footnote). However, it can be noted that the behavior of these optimal trajectories vary. It can be observed that as  $\lambda$  increases (for  $\lambda \geq 1$ ), the curvature of the desensitized trajectories reduces. For this particular example under turn radius constraints, the designer can alternatively tune the value of  $\lambda$  to obtain the desired trajectory shape.

## 4.3 The Car vs. Train Problem

Consider the 1D version of the problem described in Section 4.1, where an agent (car) is restricted to move along the x-axis, and the obstacle (train) is moving along the y-axis. Note that the dynamics for the obstacle remain the same, given in (24), while the agent dynamics takes the form

$$\dot{x}_a(t) = u(t), \quad x_a(0) = a_0,$$

where  $u(t) \in [0, v_a^{\max}]$ , and  $y_a(t) = 0, \forall t \in [0, t_f]$ . In this case, the state vector  $x = [x_a, y_o]^\top$  is two-dimensional. A schematic of the problem setup is presented in Figure 5.

Similar to the previous experiments, we assume that the agent's primary task is to minimize travel time whilst reducing risk of collision under uncertainty in the obstacle's speed. It is intuitive to expect that the desensitized solution will ensure that the distance between the train and the car is sufficiently large during the event of crossing the rail track. Computing an RCS cost using the constraint in (25) is found to provide a desensitized solution that drives the agent to reach the target point in minimum time, regardless of the distance between the agent and the obstacle (i.e, beyond the safe distance  $r_o$ ).

The discrepancy between the desensitized solution for RCS using the constraint in (25) and the intuitive solution can be understood by considering the behavior of a real-world driver. The expression in (25), although a valid constraint,

<sup>†</sup>[https://youtu.be/bf\\_fyZ9Gd4A](https://youtu.be/bf_fyZ9Gd4A)

<sup>‡</sup> $\lambda = 0.5$ : [https://youtu.be/h-c\\_IUj2I0c](https://youtu.be/h-c_IUj2I0c),  $\lambda = 2$ : [https://youtu.be/M1h\\_joVvrn0](https://youtu.be/M1h_joVvrn0),  $\lambda = 4$ : <https://youtu.be/V-mBb1gEfLM>

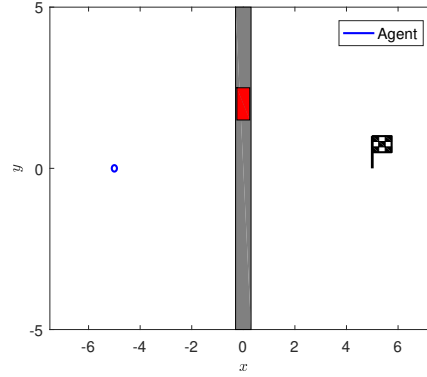


Figure 5: Schematic of the Car vs. Train problem

does not capture a driver's perception of the collision constraint in this problem. Effectively, the train's motion along the rail track is of no consequence to the driver, except when they are crossing the track. It is during this crossing phase that the driver would ensure sufficient separation (at least the safe distance  $r_o$ ) between the train and the car to prevent collision.

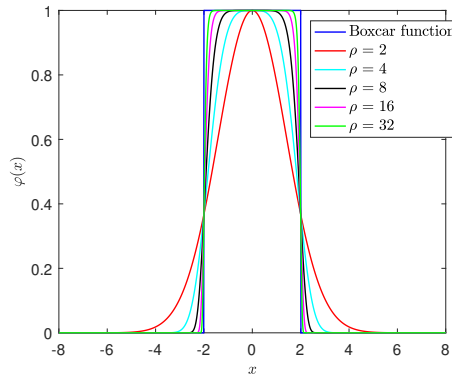


Figure 6: A super-Gaussian approximation to a Boxcar function

This motivates us to propose a constraint of the form,

$$g(x) = \mathbb{1}[|x_a(t) - x_o| \leq w_o] \underbrace{[r_o^2 - (y_a - y_o(t))^2]}_{g_y(y_o)} \leq 0, \quad (29)$$

where  $\mathbb{1}[\cdot]$  is the indicator function, and  $2w_o$  is the width of the track. Note that  $\mathbb{1}[|x_a(t) - x_o| \leq w_o]$  is a boxcar function which makes the constraint function in (29) non-smooth. To this end, we suggest the so-called *super-Gaussian* of the form

$$\varphi(x_a(t); x_o, w_o) = \exp\left(-\left[\frac{x_a(t) - x_o}{w_o}\right]^\rho\right), \quad (30)$$

where  $\rho \in 2\mathbb{Z}^+$  (set of positive even numbers), as an approximation to the boxcar function. From Figure 6, it can be observed that as  $\rho \rightarrow \infty$ ,  $\varphi$  converges to a boxcar function. Subsequently, an RCS for (29) with a super-Gaussian approximation can be obtained as

$$S_\ell = \frac{\partial}{\partial v_o} \left( \varphi(x_a(t); x_o, w_o) g_y(y_o) \right). \quad (31)$$

The results obtained by penalizing RCS in (31) are shown in Fig. 7, with simulation parameters being the same as the ones in the previous subsections except for  $\rho = 20$ ,  $v_a^{\max} = 1$ . The corresponding trajectories can be found on the web<sup>§</sup>. The video confirms that RCS (31, when penalized, does provide conservative trajectories. This exercise indicates that an appropriate constraint function is crucial for the success of the proposed approach.

<sup>§</sup><https://youtu.be/Kf6UZ0ZAhBA>



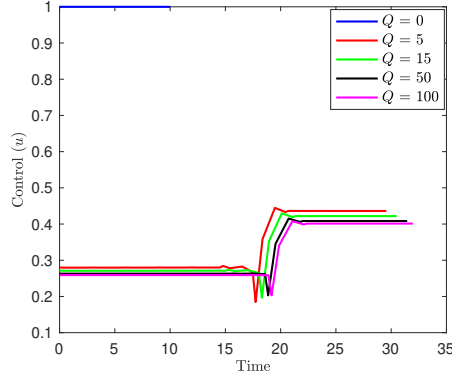


Figure 7: Optimal control for the car vs. train problem with different levels of constraint desensitization

## 5 Results and Discussion

In this section, the proposed approach is evaluated in instances involving multiple dynamic obstacles moving with uncertain velocities. The dynamics of the agent follow (22), (23). In addition to the agent's heading  $\theta$ , its speed  $v_a \in [0, 1]$  is included as a control input. Starting at location  $(0, 0)$ , the agent is tasked with reaching the target location  $(30, 0)$  in minimum time while avoiding the obstacles. We consider four different instances with the number of the obstacles  $N \in \{2, 3, 5, 10\}$ . The obstacles are all assumed to be identical and their movement is restricted to be parallel to the  $y$ -axis with their speed  $v_o$  being the uncertain parameter. The nominal value of  $v_o$  is 0.25. A schematic of the environment, containing the initial positions of the agent and the obstacles, and the directions of the obstacles' nominal velocity vectors for the case of  $N = 10$ , is shown in Figure 8.

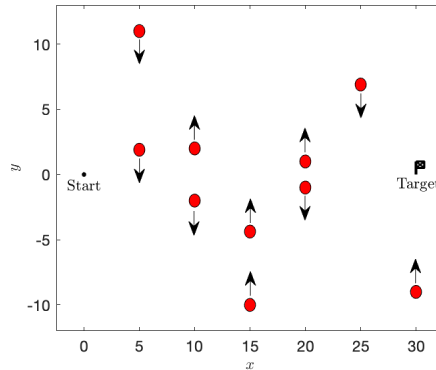


Figure 8: Schematic of an uncertain multi-obstacle environment with ten obstacles at the initial time. The red circles denote the obstacles and the arrows indicate the direction of their movement as per the nominal velocity available to the agent

Note that in each instance, there are  $N$  constraints enforcing collision avoidance, and the speed of the associated obstacle is the uncertain parameter. Ignoring zeros in the matrix  $S_\ell(t)$ , all the sensitivity terms are weighted equally by choosing  $Q$  in RCS cost of (21) to be of form  $Q = \alpha I_N$ . Each instance involves four levels of penalization on RCS cost with  $\alpha = 0$  (blue, no penalty), 0.1 (magenta), 0.33 (green), 1 (black). Visualizations for the optimal trajectories obtained by penalizing RCS, using the constraint form in (25), for different instances ( $N = 2, 3, 5, 10$ ) can be found on the web<sup>¶</sup>. From the animations, it is evident that as  $\alpha$  increases, the agent takes longer routes to avoid obstacles while maintaining a safety buffer. To characterize safety, collision probabilities are computed by running Monte Carlo (MC) simulations on the open-loop trajectory obtained from the optimal control solver (GPOPS-II) for 1000 samples. In the MC simulations, the variation in each of the obstacle's speed  $\Delta v_o$  is obtained by sampling from a normal distribution

<sup>¶</sup> $N = 2$ : <https://youtu.be/L4Qx4ta0g7I>,  $N = 3$ : <https://youtu.be/hmaHXFR6-Vo>,  $N = 5$ : <https://youtu.be/-kJ1BJEKiUo>,  $N = 10$ : <https://youtu.be/ch1EuMZDVyw>

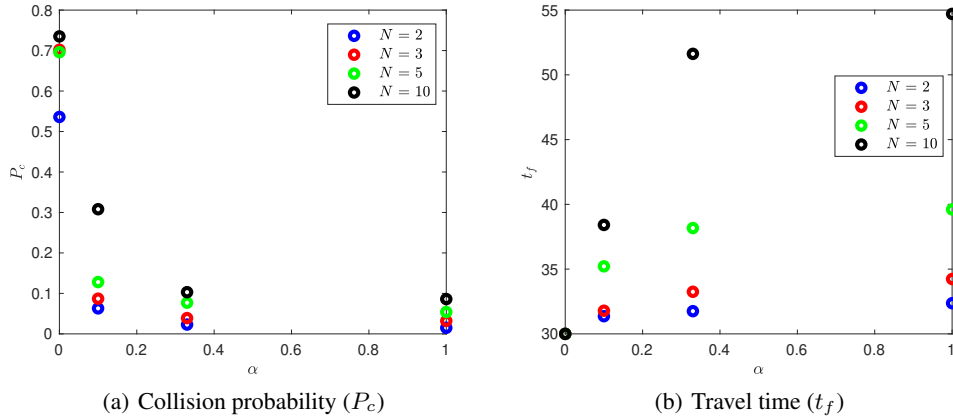


Figure 9: Trade-offs plots for instances with different number of obstacles

$N(0, \sigma^2)$ , with  $\sigma^2 = 0.1$ . The variations in the obstacles' speeds are independent of each other. The trade-off between travel times ( $t_f$ ) and collision probabilities ( $P_c$ ) for the four instances are shown in Figure 9. From Figure 9, it is seen that penalizing RCS (for higher  $\alpha$  values) yields safer trajectories that mitigate chances of constraint violation in uncertain environments while trading off optimality (travel time). For instances with  $N = 2, 3$ , a 95% reduction in collision probability is achieved for a 10% trade-off in travel time. Due to the cumulative effect of increasing obstacles and uncertain parameters on the RCS cost (that measures the risk of constraint violation), the travel times for safer trajectories are seen to increase with  $N$ .

It is observed that the compute times for the tested instances are of the same order of magnitude ( $\mathcal{O}(10^{-4})$  sec). The approach is limited by the efficiency of the chosen optimal control solver. The regularizer has no guarantees in terms of convexity, and consequently the optimizer may converge to a local minimum. Depending on the initialization, the homotopy class of the obtained trajectories may vary. For the above simulations, we report the optimal one among the trajectories obtained from different initializations. While in the above simulations, the obstacles are restricted to follow simple paths parallel to the y axis, it is important to note that the regularizer can be derived for arbitrary obstacle motion as long as its dynamics are known and the uncertain parameters are identified.

## 6 Conclusion

A sensitivity function-based regularizer is introduced to obtain conservative solutions that avoid constraint violation under parametric uncertainties in optimal control problems. Using the fact that collision avoidance can be expressed as a state constraint, the approach is applied for path planning problems involving dynamic uncertain obstacles. The proposed regularizer is first analyzed on simple toy problems to study its characteristics and to identify its limitations. It is observed that the form of the constraint function used to construct the regularizer affects the behavior of the trajectories. The results on environments with as many as ten dynamic obstacles indicate that safety can be enhanced with an acceptable trade-off in optimality using the proposed technique.

## Acknowledgments

This work has been supported by NSF award CMMI-1662542.

## References

- [1] A. K. Akametalu, J. F. Fisac, J. H. Gillula, S. Kaynama, M. N. Zeilinger, and C. J. Tomlin. Reachability-based safe learning with gaussian processes. In *IEEE Conference on Decision and Control*, pages 1424–1431, Los Angeles, CA, 2014.
- [2] G. S. Aoude, B. D. Luders, D. S. Levine, and J. P. How. Threat-aware path planning in uncertain urban environments. In *IEEE/RSJ International Conference on Intelligent Robots and Systems*, pages 6058–6063, Taipei, Taiwan, 2010.

- [3] Georges S Aoude, Brandon D Luders, Joshua M Joseph, Nicholas Roy, and Jonathan P How. Probabilistically safe motion planning to avoid dynamic obstacles with uncertain motion patterns. *Autonomous Robots*, 35(1):51–76, 2013.
- [4] C. Dabadie, S. Kaynama, and C. J. Tomlin. A practical reachability-based collision avoidance algorithm for sampled-data systems: Application to ground robots. In *IEEE/RSJ International Conference on Intelligent Robots and Systems*, pages 4161–4168, Chicago, IL, 2014.
- [5] N. E. Du Toit and J. W. Burdick. Robotic motion planning in dynamic, cluttered, uncertain environments. In *IEEE International Conference on Robotics and Automation*, pages 966–973, Anchorage, AK, 2010.
- [6] D. Fridovich-Keil, J. F. Fisac, and C. J. Tomlin. Safely probabilistically complete real-time planning and exploration in unknown environments. In *International Conference on Robotics and Automation*, pages 7470–7476, Montreal, QC, Canada, 2019.
- [7] C. Fulgenzi, A. Spalanzani, and C. Laugier. Dynamic obstacle avoidance in uncertain environment combining PVOs and occupancy grid. In *IEEE International Conference on Robotics and Automation*, pages 1610–1616, Roma, Italy, 2007.
- [8] Kris Hauser. On responsiveness, safety, and completeness in real-time motion planning. *Autonomous Robots*, 32(1):35–48, 2012.
- [9] H. K. Khalil. *Nonlinear Systems*. Prentice Hall, Third edition, 2002. Chapter 3.
- [10] S. Lengagne, N. Ramdani, and P. Fraise. Guaranteed computation of constraints for safe path planning. In *7th IEEE-RAS International Conference on Humanoid Robots*, pages 312–317, Pittsburgh, PA, 2007.
- [11] Brandon D Luders, Sertac Karaman, and Jonathan P How. Robust sampling-based motion planning with asymptotic optimality guarantees. In *AIAA Guidance, Navigation, and Control Conference*, Boston, MA, 2013.
- [12] Y. Luo, P. Cai, A. Bera, D. Hsu, W. S. Lee, and D. Manocha. PORCA: Modeling and planning for autonomous driving among many pedestrians. *IEEE Robotics and Automation Letters*, 3(4):3418–3425, Oct 2018.
- [13] V. R. Makkapati, M. Dor, and P. Tsiotras. Trajectory desensitization in optimal control problems. In *IEEE Conference on Decision and Control*, pages 2478–2483, Miami, FL, 2018.
- [14] V. R. Makkapati, D. Maity, M. Dor, and P. Tsiotras. C-DOC: Co-state desensitized optimal control. *arXiv preprint arXiv:1910.00046*, 2019.
- [15] M. C. Mora and J. Tornero. Path planning and trajectory generation using multi-rate predictive artificial potential fields. In *IEEE/RSJ International Conference on Intelligent Robots and Systems*, pages 2990–2995, Nice, France, 2008.
- [16] M. A. Patterson and A. V. Rao. GPOPS-II: A MATLAB software for solving multiple-phase optimal control problems using hp-adaptive Gaussian quadrature collocation methods and sparse nonlinear programming. *ACM Trans. Mathematical Software*, 41(1):1:1–1:37, October 2014.
- [17] Mohammadhussein Rafieisakhaei, Suman Chakravorty, and PR Kumar. Non-Gaussian SLAP: Simultaneous localization and planning under non-Gaussian uncertainty in static and dynamic environments. *arXiv preprint arXiv:1605.01776*, 2016.
- [18] Haijun Shen, Hans Seywald, and Richard W Powell. Desensitizing the minimum-fuel powered descent for mars pinpoint landing. *Journal of guidance, control, and dynamics*, 33(1):108–115, 2010.
- [19] Sebastian Thrun, Wolfram Burgard, and Dieter Fox. *Probabilistic Robotics*. MIT press Cambridge, 2000.
- [20] J. van den Berg, D. Ferguson, and J. Kuffner. Anytime path planning and replanning in dynamic environments. In *IEEE International Conference on Robotics and Automation*, pages 2366–2371, Orlando, FL, 2006.
- [21] Jur van den Berg, Pieter Abbeel, and Ken Goldberg. LQG-MP: Optimized path planning for robots with motion uncertainty and imperfect state information. *The International Journal of Robotics Research*, 30(7):895–913, 2011.
- [22] W. Xu, J. Pan, J. Wei, and J. M. Dolan. Motion planning under uncertainty for on-road autonomous driving. In *IEEE International Conference on Robotics and Automation*, pages 2507–2512, Hong Kong, China, 2014.
- [23] Cheng Zhang and Amin Hammad. Improving lifting motion planning and re-planning of cranes with consideration for safety and efficiency. *Advanced Engineering Informatics*, 26(2):396–410, 2012.
- [24] Q. Zhu. Hidden Markov model for dynamic obstacle avoidance of mobile robot navigation. *IEEE Transactions on Robotics and Automation*, 7(3):390–397, June 1991.
- [25] M. Zucker, J. Kuffner, and M. Branicky. Multipartite RRTs for rapid replanning in dynamic environments. In *IEEE International Conference on Robotics and Automation*, pages 1603–1609, Roma, Italy, 2007.